International Journal of Pure and Applied Mathematics
Volume 37 No. 3 2007, 395-422

EIGENSTRUCTURE OF THE EQUILATERAL TRIANGLE PART IV: THE ABSORBING BOUNDARY

Brian J. M^{c}Cartin
Department of Applied Mathematics
Kettering University
1700 West Third Avenue, Flint, MI 48504-4898, USA
e-mail: bmccarti@kettering.edu

Abstract: Lamé's formulas for the eigenvalues and eigenfunctions of the Laplacian on an equilateral triangle under Dirichlet and Neumann boundary conditions are herein extended to the Robin problem with an absorbing boundary condition. They are shown to form a complete orthogonal system. Various properties of the spectrum and modal functions are explored.

AMS Subject Classification: 35C05, 35J05, 35P10
Key Words: equilateral triangle, Laplacian eigenvalues/eigenvectors, Robin problem, absorbing boundary condition

1. Introduction

The eigenstructure of the Laplacian on an equilateral triangle under either Dirichlet or Neumann boundary conditions was explicitly determined by Lamé [3, 4] in the context of his studies of heat transfer in polyhedral bodies and then further explored by Pockels [11]. However, Lamé and subsequent researchers such as Pockels did not provide a complete derivation of these formulas but rather simply stated them and then proceeded to show that they satisfied the relevant differential equation and associated boundary condition. Such a complete, direct, and elementary derivation of Lamé's formulas has only recently been provided for the Dirichlet problem [7] as well as the Neumann problem, [8]. This was subsequently extended to the Robin problem with a radiation boundary condition [9].

Received: April 4, 2007

It is the express purpose of the present work to extend this recent work to the much more difficult case of the Robin problem with an absorbing boundary condition. The principal analytical difficulty that must be overcome is that, unlike the case of a radiation boundary condition, the eigenvalues, while still real, may now be negative. The presence of these negative eigenvalues has the unfortunate consequence of destroying the natural homotopy between Lamé's Neumann and Dirichlet modes which was so heavily exploited in the prior investigation of the radiation boundary condition, [9].

We commence by employing separation of variables in Lamé's natural triangular coordinate system to derive the eigenvalues and eigenfunctions of the Robin problem with an absorbing boundary condition (ABC). An important feature of this derivation is the decomposition into symmetric and antisymmetric modes (eigenfunctions). The problem is then reduced to the solution of a system of transcendental equations which we treat numerically using *Matlab*. Surprisingly, all of the modes so determined (henceforth dubbed ABC modes) are expressible as combinations of either trigonometric or hyperbolic sines and cosines.

A natural homotopy between Lamé's Neumann modes and the ABC modes is exploited not only in the derivation of the modes but is also employed to shed light on the properties of these newly derived modes. Prominent among these considerations is rotational symmetry and modal degeneracy, [10]. It is observed that the arguments presented in [9] for orthogonality and completeness in the case of a radiation boundary condition are likewise applicable in the case of an absorbing boundary condition.

This natural homotopy from Lamé's Neumann modes to the ABC modes possesses a bipartite structure. On the one hand, for ABC modes corresponding to eigenvalues that always remain positive, the homotopy may be extended to approach Lamé's Dirichlet modes. On the other hand, ABC modes corresponding to eigenvalues that eventually become negative do not approach Dirichlet modes. The determination of the precise nature of these latter eigenvalues together with that of their corresponding eigenfunctions is the primary focus of the present study.

2. The Robin Eigenproblem for the Equilateral Triangle

In the course of his investigations into the cooling of a right prism with equilateral triangular base [3, 4], Lamé was lead to consider the eigenvalue problem

$$\Delta T(x,y) + k^2 T(x,y) = 0,\ (x,y) \in \tau; \quad \frac{\partial T}{\partial \nu}(x,y) + \sigma T(x,y) = 0, \\ (x,y) \in \partial\tau\,, \quad (1)$$

where Δ is the two-dimensional Laplacian, $\frac{\partial^2}{\partial x^2} + \frac{\partial^2}{\partial y^2}$, τ is the equilateral triangle shown in Figure 1, ν is its outward pointing normal, and σ is a material parameter. Lamé later encountered the same eigenproblem when considering the vibrational modes of an elastic membrane stretched over an equilateral triangle, [5]. We shall find through the ensuing analysis that all of the eigenfunctions (modes) of this problem are expressible in terms of either trigonometric or hyperbolic sines and cosines.

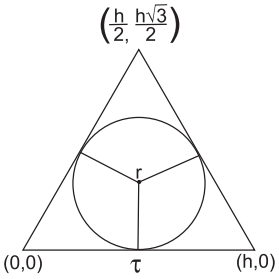

Figure 1: Equilateral triangle with incircle

The boundary condition in equation (1) with $\sigma > 0$ arises when heat dissipates from a body into a surrounding medium by a combination of convection, radiation and conduction. It also appears in the study of the vibrational modes of an elastic membrane. This case of the so-called radiation boundary condition, which is self-adjoint with k^2 real and nonnegative, received exhaustive treatment in [9].

When $\sigma < 0$, this boundary condition corresponds to the absorption of energy, [13]. It is this case of the so-called absorbing boundary condition (ABC), which is still self-adjoint so that k^2 is again real but may now be negative, that is the subject of the present paper. If σ is allowed to be complex (which is prohibited herein) then the identical problem occurs also in wave propagation in acoustic ducts and electromagnetic waveguides. This problem, which is no longer self-adjoint so that k^2 may now be complex, will be taken up in the final installment of this series of papers on the eigenstructure of the equilateral triangle.

Observe that in equation (1) when $\sigma \to 0^-$ we recover the Neumann problem, [8]. Thus, we may profitably view σ as a continuation parameter which provides a homotopy extending from this well understood problem to that of

the absorbing boundary condition. Throughout the ensuing development we will avail ourselves of this important observation.

Furthermore, note that *if the normal derivative remains bounded* then $\sigma \to -\infty$ yields the Dirichlet problem, [7]. In that case, the homotopy may be further extended to lead from a Neumann mode to a corresponding Dirichlet mode. For the radiation boundary condition this is always the case [9], while for the absorbing boundary condition only sometimes so.

3. Triangular Coordinate System

Reconsider the equilateral triangle of side h in standard position in Cartesian coordinates (x, y) (Figure 1) and define the *triangular coordinates* (u, v, w) of a point P (Figure 2) by

$$\begin{aligned} u &= r - y\,, \\ v &= \frac{\sqrt{3}}{2} \cdot (x - \frac{h}{2}) + \frac{1}{2} \cdot (y - r)\,, \\ w &= \frac{\sqrt{3}}{2} \cdot (\frac{h}{2} - x) + \frac{1}{2} \cdot (y - r)\,, \end{aligned} \tag{2}$$

where $r = h/(2\sqrt{3})$ is the inradius of the triangle. The coordinates u, v, w may be described as the distances of the triangle center to the projections of the point onto the altitudes, measured positively toward a side and negatively toward a vertex.

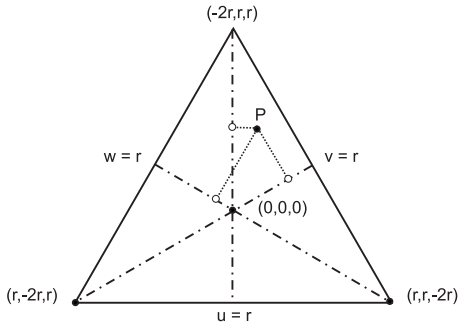

Figure 2: Triangular coordinate system

Note that Lamé's triangular coordinates satisfy the relation

$$u + v + w = 0. \tag{3}$$

Moreover, the center of the triangle has coordinates $(0, 0, 0)$ and the three sides

of the triangle are given by $u = r$, $v = r$, and $w = r$, thus simplifying the application of boundary conditions. They are closely related to the barycentric coordinates (U, V, W) introduced by his contemporary A.F. Möbius in 1827, see [2]:

$$U = \frac{r-u}{3r}, \quad V = \frac{r-v}{3r}, \quad W = \frac{r-w}{3r}\,, \tag{4}$$

satisfying $U + V + W = 1$. These were destined to become the darling of finite element practitioners in the 20-th century.

4. Separation of Variables

We now commence with our original, complete, and elementary derivation by introducing the orthogonal coordinates (ξ, η) given by

$$\xi = u, \ \eta = v - w. \tag{5}$$

Equation (1) becomes

$$\frac{\partial^2 T}{\partial \xi^2} + 3\frac{\partial^2 T}{\partial \eta^2} + k^2 T = 0. \tag{6}$$

Hence, if we seek a separated solution of the form

$$f(\xi) \cdot g(\eta) \tag{7}$$

we arrive at

$$f'' + \alpha^2 f = 0; \quad g'' + \beta^2 g = 0; \quad \alpha^2 + 3\beta^2 = k^2. \tag{8}$$

Thus, there exist separated solutions of the form

$$f(u) \cdot g(v - w), \tag{9}$$

where f and g are (possibly complex) trigonometric functions. The only restriction in the above is that k^2 and T be real.

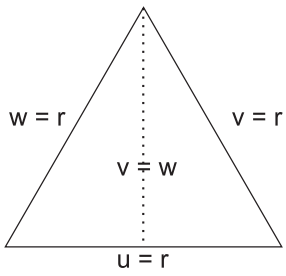

Figure 3: Modal line of symmetry/antisymmetry

Before proceeding any further, we will decompose the sought after eigenfunction into parts symmetric and antisymmetric about the altitude $v = w$ (see

Figure 3)

$$T(u,v,w) = T_s(u,v,w) + T_a(u,v,w), \tag{10}$$

where

$$\begin{aligned} T_s(u,v,w) &= \frac{T(u,v,w)+T(u,w,v)}{2}; \\ T_a(u,v,w) &= \frac{T(u,v,w)-T(u,w,v)}{2}, \end{aligned} \tag{11}$$

henceforth to be dubbed a symmetric/antisymmetric mode, respectively. We next take up the determination of T_s and T_a.

5. Construction of Symmetric/Antisymmetric Modes

As shown elsewhere, a sum of three terms of the form of equation (9) is required to solve the Robin problem, [9]. Hence, we make the Ansatz:

$$\begin{aligned} T_s &= \cos[\frac{\pi\lambda}{3r}(u+2r)-\delta_1]\cdot\cos[\frac{\pi(\mu-\nu)}{9r}(v-w)] \\ &+ \cos[\frac{\pi\mu}{3r}(u+2r)-\delta_2]\cdot\cos[\frac{\pi(\nu-\lambda)}{9r}(v-w)] \\ &+ \cos[\frac{\pi\nu}{3r}(u+2r)-\delta_3]\cdot\cos[\frac{\pi(\lambda-\mu)}{9r}(v-w)], \end{aligned} \tag{12}$$

$$\begin{aligned} T_a &= \cos[\frac{\pi\lambda}{3r}(u+2r)-\delta_1]\cdot\sin[\frac{\pi(\mu-\nu)}{9r}(v-w)] \\ &+ \cos[\frac{\pi\mu}{3r}(u+2r)-\delta_2]\cdot\sin[\frac{\pi(\nu-\lambda)}{9r}(v-w)] \\ &+ \cos[\frac{\pi\nu}{3r}(u+2r)-\delta_3]\cdot\sin[\frac{\pi(\lambda-\mu)}{9r}(v-w)], \end{aligned} \tag{13}$$

with

$$\lambda+\mu+\nu = 0, \tag{14}$$

and eigenvalue

$$k^2 = \frac{2}{27}(\frac{\pi}{r})^2[\lambda^2+\mu^2+\nu^2] = \frac{4}{27}(\frac{\pi}{r})^2[\mu^2+\mu\nu+\nu^2]. \tag{15}$$

As we shall see, the symmetric mode never vanishes identically while the antisymmetric mode may.

Careful perusal of equations (12) and (13) now reveals that for $\delta_1 = \delta_2 = \delta_3 = 0$ they reduce to the symmetric/antisymmetric modes of the Neumann problem [8] while for $\delta_1 = 3\pi/2,\ \delta_2 = -\pi/2,\ \delta_3 = -\pi/2$ they reduce to the symmetric/antisymmetric modes of the Dirichlet problem, [7]. Thus, our task amounts to finding values of $\lambda,\ \mu,\ \nu,\ \delta_1,\ \delta_2,\ \delta_3$ so that the Robin boundary condition is satisfied along the periphery of the equilateral triangle. These

values are to satisfy the constraints that k^2, T_s and T_a must be real as well as equation (14).

Imposition of the Robin boundary condition along $u = r$ yields

$$\tan(\pi\lambda - \delta_1) = \frac{3\sigma r}{\pi\lambda},\ \tan(\pi\mu - \delta_2) = \frac{3\sigma r}{\pi\mu},\ \tan(\pi\nu - \delta_3) = \frac{3\sigma r}{\pi\nu}, \tag{16}$$

while imposition along $v = r$ yields

$$\tan(-\frac{\delta_2+\delta_3}{2}) = \frac{3\sigma r}{\pi\lambda},\ \tan(-\frac{\delta_3+\delta_1}{2}) = \frac{3\sigma r}{\pi\mu},\ \tan(-\frac{\delta_1+\delta_2}{2}) = \frac{3\sigma r}{\pi\nu}. \tag{17}$$

By symmetry/antisymmetry, the boundary condition along $w = r$ will thereby be automatically satisfied.

Introducing the auxiliary variables, $L,\ M,\ N$, while collecting together these equations produces

$$\begin{aligned}
\tan(\pi\lambda - \delta_1) = \tan(-\frac{\delta_2+\delta_3}{2}) = \frac{3\sigma r}{\pi\lambda} = \tan L, \quad L := -\frac{\delta_2+\delta_3}{2}, \\
\tan(\pi\mu - \delta_2) = \tan(-\frac{\delta_3+\delta_1}{2}) = \frac{3\sigma r}{\pi\mu} = \tan M, \quad M := -\frac{\delta_3+\delta_1}{2}, \\
\tan(\pi\nu - \delta_3) = \tan(-\frac{\delta_1+\delta_2}{2}) = \frac{3\sigma r}{\pi\nu} = \tan N, \quad N := -\frac{\delta_1+\delta_2}{2},
\end{aligned} \tag{18}$$

and these six equations may in turn be reduced to the solution of the system of three transcendental equations for $L,\ M,\ N$

$$\begin{aligned}
[2L - M - N - (m+n)\pi]\cdot\tan L &= 3\sigma r, \\
[2M - N - L + m\pi]\cdot\tan M &= 3\sigma r, \\
[2N - L - M + n\pi]\cdot\tan N &= 3\sigma r,
\end{aligned} \tag{19}$$

where $m = 0, 1, 2, \ldots,\ n = m, m+1, \ldots$.

Once $L,\ M,\ N$ have been numerically approximated, e.g. using *Matlab*, the parameters of primary interest may then be determined as

$$\delta_1 = L - M - N; \quad \delta_2 = -L + M - N; \quad \delta_3 = -L - M + N, \tag{20}$$

and

$$\lambda = -\mu - \nu; \quad \mu = \frac{2M - N - L}{\pi} + m; \quad \nu = \frac{2N - L - M}{\pi} + n. \tag{21}$$

For future reference, when $m = n$ we have $M = N$, $\delta_2 = \delta_3$, $\mu = \nu$, and $2\pi\mu = \delta_2 - \delta_1 + 2m\pi$.

Of particular interest is the limit $\sigma \to 0^-$, where we find that L, M, N each approach 0, as do $\delta_1, \delta_2, \delta_3$, and, most significantly, $\lambda \to -(m+n), \mu \to m, \nu \to n$. In other words, we recover in this limit the Neumann modes. Thus, we have constructed a homotopy extending from each ABC mode back to the Neumann mode with the same index (m, n) as $\sigma \to 0^-$. The behavior of the ABC modes as $\sigma \to -\infty$ is more subtle and will be addressed once we have established some of their basic properties.

6. Modal Properties

Certain properties of the ABC modes follow directly from equations (12) and (13). However, these equations are identical to those for the radiation boundary condition, [9], except that some quantities may now be complex so long as k^2, T_s and T_a are real. Thus, their proofs are formally identical to those of [9] and for that reason they are omitted here.

In what follows, it will be convenient to have the following alternative representations of our ABC modes

$$\begin{aligned} T_s^{m,n} = \frac{1}{2} \quad \{ \quad & \cos[\frac{2\pi}{9r}(\lambda u + \mu v + \nu w + 3\lambda r) - \delta_1] \\ + \quad & \cos[\frac{2\pi}{9r}(\nu u + \mu v + \lambda w + 3\nu r) - \delta_3] \\ + \quad & \cos[\frac{2\pi}{9r}(\mu u + \nu v + \lambda w + 3\mu r) - \delta_2] \\ + \quad & \cos[\frac{2\pi}{9r}(\mu u + \lambda v + \nu w + 3\mu r) - \delta_2] \\ + \quad & \cos[\frac{2\pi}{9r}(\nu u + \lambda v + \mu w + 3\nu r) - \delta_3] \\ + \quad & \cos[\frac{2\pi}{9r}(\lambda u + \nu v + \mu w + 3\lambda r) - \delta_1]\}, \end{aligned} \tag{22}$$

$$\begin{aligned} T_a^{m,n} = \frac{1}{2} \quad \{ \quad & \sin[\frac{2\pi}{9r}(\lambda u + \mu v + \nu w + 3\lambda r) - \delta_1] \\ - \quad & \sin[\frac{2\pi}{9r}(\nu u + \mu v + \lambda w + 3\nu r) - \delta_3] \\ + \quad & \sin[\frac{2\pi}{9r}(\mu u + \nu v + \lambda w + 3\mu r) - \delta_2] \\ - \quad & \sin[\frac{2\pi}{9r}(\mu u + \lambda v + \nu w + 3\mu r) - \delta_2] \\ + \quad & \sin[\frac{2\pi}{9r}(\nu u + \lambda v + \mu w + 3\nu r) - \delta_3] \\ - \quad & \sin[\frac{2\pi}{9r}(\lambda u + \nu v + \mu w + 3\lambda r) - \delta_1]\}, \end{aligned} \tag{23}$$

obtained from equation (12) and equation (13), respectively, by the application of appropriate trigonometric identities.

We may pare the collection of antisymmetric Robin modes through the following observation.

Theorem 1. *$T_s^{m,n}$ never vanishes identically while $T_a^{m,n}$ vanishes identically if and only if m=n.*

Hence, our reduced modal system is $\{T_s^{m,n}\ (n \geq m \geq 0);\ T_a^{m,n}\ (n > m \geq$

$0)\}$.

We next give the case $m = n$ further consideration. Recall that we have just determined that $T_a^{m,m} \equiv 0$. Furthermore, in this case, we may combine the terms of equation (22) to yield

$$T_s^{m,m} = \cos[\frac{2\pi\mu}{3r}(r-u) - \delta_2] + \cos[\frac{2\pi\mu}{3r}(r-v) - \delta_2] + \cos[\frac{2\pi\mu}{3r}(r-w) - \delta_2], \quad (24)$$

which clearly illustrates that any permutation of (u, v, w) leaves $T_s^{m,m}$ invariant. This is manifested geometrically in the invariance of $T_s^{m,m}$ under a 120° rotation about the triangle center. This invariance will henceforth be termed rotational symmetry.

Moreover, the modes $T_s^{m,m}$ are not the only ones that are rotationally symmetric.

Theorem 2. *$T_s^{m,n}$ and $T_a^{m,n}$ are rotationally symmetric if and only if $m \equiv n$ (mod3).*

7. The Limit $\sigma \to -\infty$

In the case of the radiation boundary condition ($\sigma > 0$) [9], the (m, n) Neumann mode [8] "morphs" analytically into the $(m+1, n+1)$ Dirichlet mode [7] as σ ranges from 0 to ∞. This suggests that in the case of the absorbing boundary condition ($\sigma < 0$), the (m, n) Neumann mode might "morph" analytically into the $(m-1, n-1)$ Dirichlet mode as σ ranges from 0 to $-\infty$.

However, the complete set of Neumann modes is given by $\{N_s^{m,n}\ (n \geq m \geq 0);\ N_a^{m,n}\ (n > m \geq 0)\}$ while the complete set of Dirichlet modes is given by $\{D_s^{m,n}\ (n \geq m > 0);\ D_a^{m,n}\ (n > m > 0)\}$. Thus, the above conjectured behavior of the ABC modes, $\{T_s^{m,n}\ (n \geq m \geq 0);\ T_a^{m,n}\ (n > m \geq 0)\}$, as $\sigma \to -\infty$, while feasible for $m \geq 2$ (the "ABC-Dirichlet modes"), is insufficient in the case of $m = 0, 1$ (the "missing modes"). Consequently, we next investigate these cases individually.

7.1. The ABC-Dirichlet Modes

The case $m \geq 2$ closely parallels that of the radiation boundary condition, [9]. Specifically, as $\sigma \to -\infty$, we find that $L \to \pi/2, M \to -\pi/2, N \to -\pi/2$ and $\delta_1 \to 3\pi/2, \delta_2 \to -\pi/2, \delta_3 \to -\pi/2$, and, most significantly, $\lambda \to 2 -$

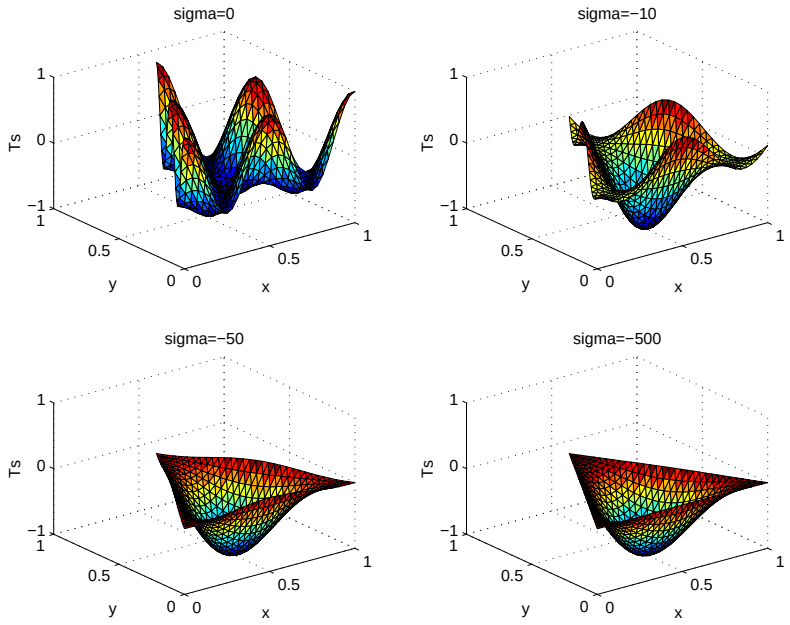

Figure 4: $(2,2)$ Symmetric mode

$(m+n), \mu \to m-1, \nu \to n-1$. In other words, we recover in this limit the Dirichlet modes. Thus, we have successfully constructed a homotopy leading from the ABC-Dirichlet modes to the Dirichlet modes. Moreover, we have indexed our ABC-Dirichlet modes in correspondence with the corresponding Neumann modes with the result that, as σ ranges from 0 to $-\infty$, the (m,n) ABC-Dirichlet mode "morphs" continuously (in fact, analytically!) from the (m,n) Neumann mode into the $(m-1,n-1)$ Dirichlet mode.

Figure 4 shows the $(2,2)$ Neumann mode morphing into the fundamental $(1,1)$ Dirichlet mode. In this and all subsequent figures, we set $h=1$. By Theorem 1, there is no antisymmetric mode and, by Theorem 2, the symmetric mode is rotationally symmetric. Figures 5 and 6 correspondingly display the $(2,3)$ symmetric and antisymmetric modes, respectively. By Theorem 1, there are indeed both symmetric and antisymmetric modes and, by Theorem 2, neither of them is rotationally symmetric. In these and all subsequent plots, the modes have been normalized so that their maximum absolute value is unity. This elegant treatment of the ABC-Dirichlet modes begs the question: "What happens to the missing $m=0,1$ modes as $\sigma \to -\infty$?"

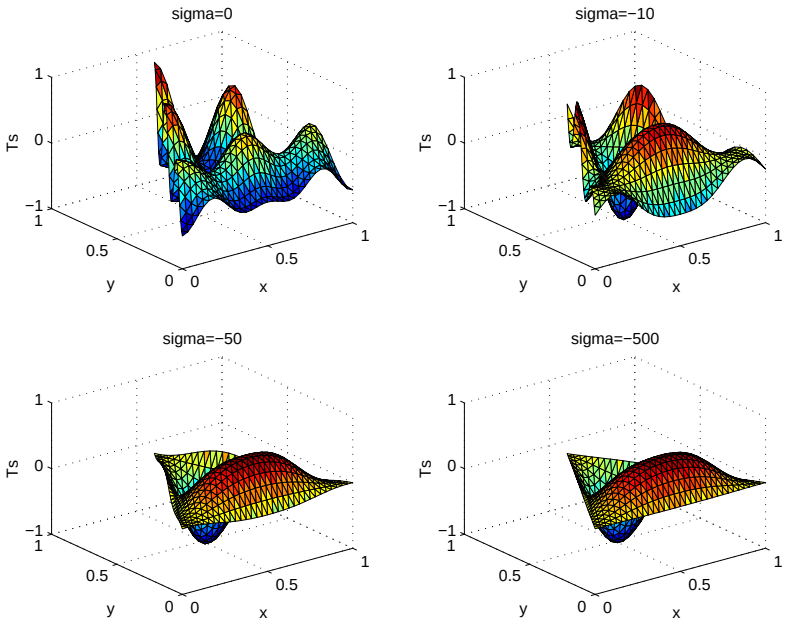

Figure 5: $(2,3)$ Symmetric mode

7.2. The Missing Modes

The solution to the mystery of the missing modes naturally decomposes into four special cases each of which we now explore separately.

7.2.1. The $(0,0)$ Mode

For $\sigma < 0$, all the parameters of Section 5 become pure imaginary:

$$\lambda = \lambda^I \cdot \imath, \quad \mu = \mu^I \cdot \imath, \quad \nu = \nu^I \cdot \imath, \tag{25}$$

$$\delta_1 = \delta_1^I \cdot \imath, \quad \delta_2 = \delta_2^I \cdot \imath, \quad \delta_3 = \delta_3^I \cdot \imath, \tag{26}$$

$$L = L^I \cdot \imath, \quad M = M^I \cdot \imath, \quad N = N^I \cdot \imath. \tag{27}$$

Equation (12) becomes

$$\begin{aligned} T_s &= \cosh[\frac{\pi\lambda^I}{3r}(u+2r) - \delta_1^I] \cdot \cosh[\frac{\pi(\mu^I - \nu^I)}{9r}(v-w)] \\ &+ \cosh[\frac{\pi\mu^I}{3r}(u+2r) - \delta_2^I] \cdot \cosh[\frac{\pi(\nu^I - \lambda^I)}{9r}(v-w)] \end{aligned} \tag{28}$$

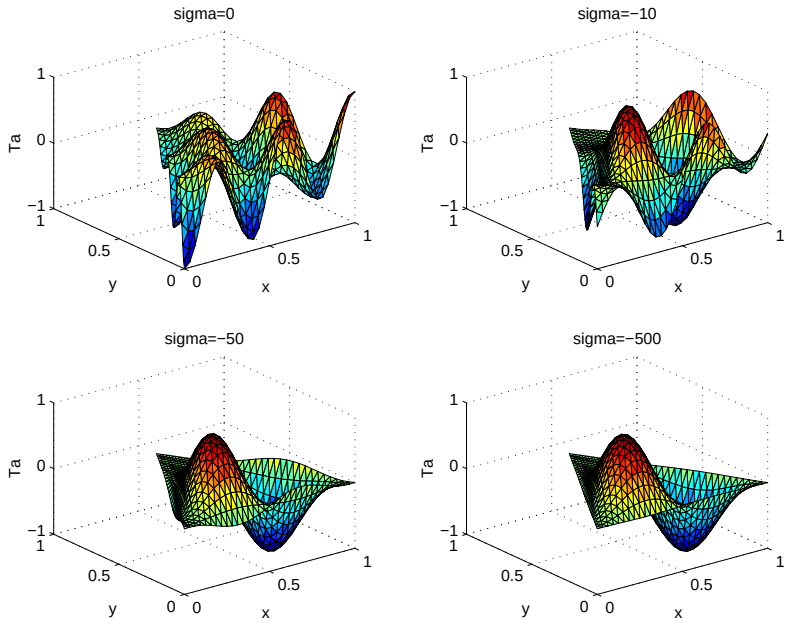

Figure 6: $(2,3)$ Antisymmetric mode

$$+ \quad \cosh[\frac{\pi\nu^I}{3r}(u+2r)-\delta_3^I]\cdot\cosh[\frac{\pi(\lambda^I-\mu^I)}{9r}(v-w)],$$

with

$$\lambda^I+\mu^I+\nu^I=0, \tag{29}$$

and eigenvalue

$$k^2=-\frac{2}{27}(\frac{\pi}{r})^2[(\lambda^I)^2+(\mu^I)^2+(\nu^I)^2]=-\frac{4}{27}(\frac{\pi}{r})^2[(\mu^I)^2+\mu^I\cdot\nu^I+(\nu^I)^2]. \tag{30}$$

Equations (19) become

$$\begin{aligned}[2L^I-M^I-N^I]\cdot\tanh L^I &= -3\sigma r,\\ [2M^I-N^I-L^I]\cdot\tanh M^I &= -3\sigma r,\\ [2N^I-L^I-M^I]\cdot\tanh N^I &= -3\sigma r.\end{aligned} \tag{31}$$

Finally, equations (20) become

$$\delta_1^I=L^I-M^I-N^I;\ \delta_2^I=-L^I+M^I-N^I;\ \delta_3^I=-L^I-M^I+N^I, \tag{32}$$

and equations (21) become

$$\lambda^I=-\mu^I-\nu^I;\ \mu^I=\frac{2M^I-N^I-L^I}{\pi};\ \nu^I=\frac{2N^I-L^I-M^I}{\pi}. \tag{33}$$

Furthermore, we have $M^I=N^I$, $\delta_2^I=\delta_3^I=-L^I$, and $\mu^I=\nu^I$. Asymptoti-

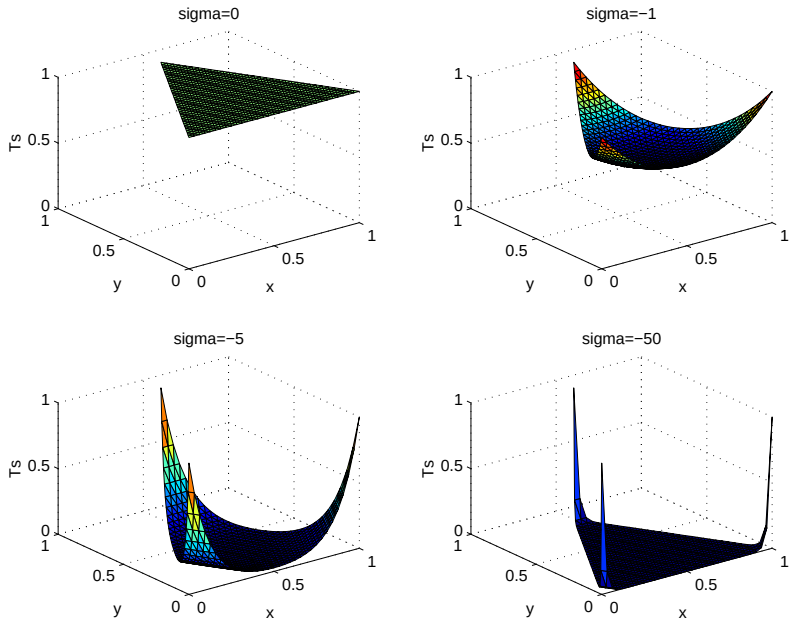

Figure 7: $(0,0)$ Symmetric mode

cally, as $\sigma \to -\infty$, we have the limiting values:

$$L^I = -\delta_2^I = -\delta_3^I \to \tanh^{-1}(1/2), \tag{34}$$

$$M^I = N^I \to \tanh^{-1}(1/2) + 3\sigma r, \tag{35}$$

$$\delta_1^I \to -\tanh^{-1}(1/2) - 6\sigma r, \tag{36}$$

$$\mu^I = \nu^I \to \frac{3\sigma r}{\pi} \Rightarrow k^2 \to -4\sigma^2. \tag{37}$$

Equation (28) for $T_s^{0,0}(u,v,w)$ becomes unbounded as $\sigma \to -\infty$. However, if we first scale it by its value at a vertex, $T_s^{0,0}(r,-2r,r)$, we find that this normalized mode approaches 1 at the three vertices and 0 elsewhere. Such singular limiting behavior, necessary since this does not approach a Dirichlet mode, is on display in Figure 7.

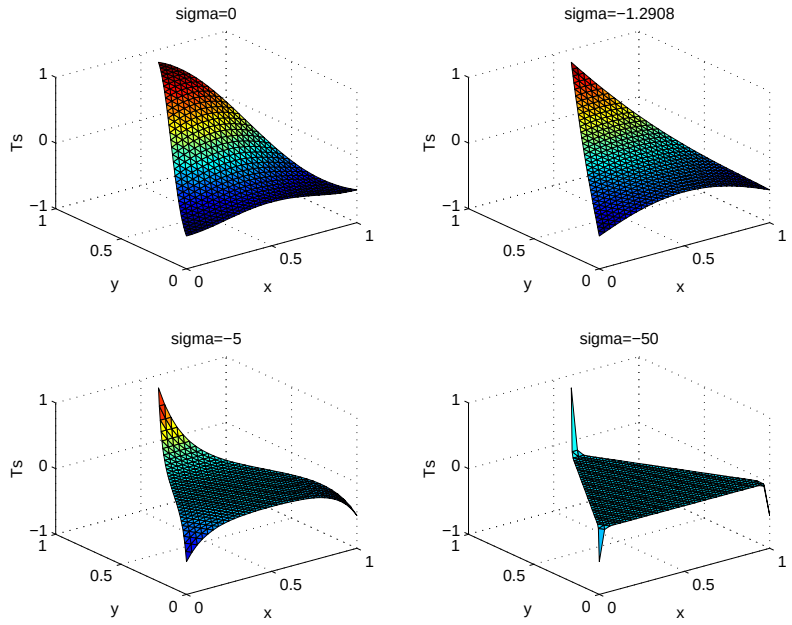

Figure 8: $(0,1)$ Symmetric mode

7.2.2. The $(0, n \geq 1)$ Modes

For $\sigma < 0$, μ becomes pure imaginary, and the remaining parameters of Section 5 become complex in such a way so as to guarantee that k^2, T_s and T_a are real:

$$\lambda = -\nu^R - \frac{\mu^I}{2} \cdot \imath, \quad \mu = \mu^I \cdot \imath, \quad \nu = \nu^R - \frac{\mu^I}{2} \cdot \imath, \tag{38}$$

$$\delta_1 = -\delta_3^R + \delta_3^I \cdot \imath, \quad \delta_2 = \delta_2^I \cdot \imath, \quad \delta_3 = \delta_3^R + \delta_3^I \cdot \imath, \tag{39}$$

$$L = -N^R + N^I \cdot \imath, \quad M = M^I \cdot \imath, \quad N = N^R + N^I \cdot \imath. \tag{40}$$

Note that

$$\lambda + \mu + \nu = 0. \tag{41}$$

Now, the middle term of equation (12), (13) is real while the outer terms are complex conjugates so that these equations may be recast in the real form

$$\begin{aligned} T_s &= \cosh[\frac{\pi\mu^I}{3r}(u+2r) - \delta_2^I] \cdot \cos[\frac{2\pi\nu^R}{9r}(v-w)] \\ &+ 2 \cdot \cosh[\frac{\pi\mu^I}{6r}(u+2r) + \delta_3^I] \cdot \cosh[\frac{\pi\mu^I}{6r}(v-w)] \end{aligned} \tag{42}$$

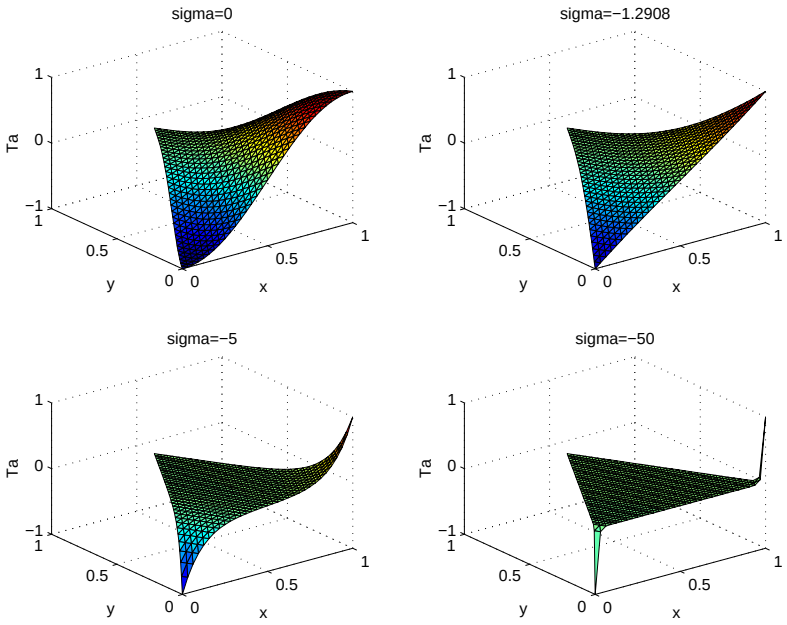

Figure 9: $(0,1)$ Antisymmetric mode

$$
\begin{aligned}
& \cdot\cos[\frac{\pi\nu^R}{3r}(u+2r)-\delta_3^R]\cdot\cos[\frac{\pi\nu^R}{9r}(v-w)] \\
+\ & 2\cdot\sinh[\frac{\pi\mu^I}{6r}(u+2r)+\delta_3^I]\cdot\sinh[\frac{\pi\mu^I}{6r}(v-w)] \\
& \cdot\sin[\frac{\pi\nu^R}{3r}(u+2r)-\delta_3^R]\cdot\sin[\frac{\pi\nu^R}{9r}(v-w)], \\
T_a\ =\ & \cosh[\frac{\pi\mu^I}{3r}(u+2r)-\delta_2^I]\cdot\sin[\frac{2\pi\nu^R}{9r}(v-w)] \\
+\ & 2\cdot\cosh[\frac{\pi\mu^I}{6r}(u+2r)+\delta_3^I]\cdot\cosh[\frac{\pi\mu^I}{6r}(v-w)] \\
& \cdot\cos[\frac{\pi\nu^R}{3r}(u+2r)-\delta_3^R]\cdot\sin[\frac{\pi\nu^R}{9r}(v-w)] \\
-\ & 2\cdot\sinh[\frac{\pi\mu^I}{6r}(u+2r)+\delta_3^I]\cdot\sinh[\frac{\pi\mu^I}{6r}(v-w)] \\
& \cdot\sin[\frac{\pi\nu^R}{3r}(u+2r)-\delta_3^R]\cdot\cos[\frac{\pi\nu^R}{9r}(v-w)].
\end{aligned}
\tag{43}
$$

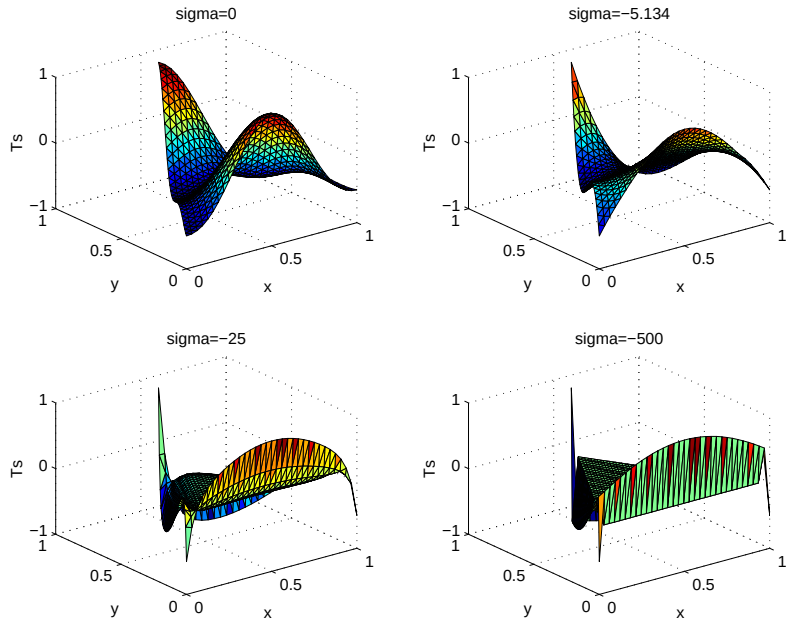

Figure 10: $(0, 2)$ Symmetric mode

with eigenvalue

$$k^2 = \frac{4}{27}(\frac{\pi}{r})^2[(\nu^R)^2 - \frac{3}{4}(\mu^I)^2]. \tag{44}$$

Equations (19) become

$$-2(M^I - N^I)\cdot \tanh M^I = 3\sigma r,$$

$$\frac{(3N^R + n\pi)\sin(N^R)\cos(N^R) - (N^I - M^I)\sinh(N^I)\cosh(N^I)}{\cos^2(N^R)\cosh^2(N^I) + \sin^2(N^R)\sinh^2(N^I)} = 3\sigma r,$$

$$\frac{(N^I - M^I)\sin(N^R)\cos(N^R) + (3N^R + n\pi)\sinh(N^I)\cosh(N^I)}{\cos^2(N^R)\cosh^2(N^I) + \sin^2(N^R)\sinh^2(N^I)} = 0. \tag{45}$$

Finally, equations (20) become

$$\delta_1 = -2N^R - M^I\cdot \imath; \quad \delta_2 = (M^I - 2N^I)\cdot \imath; \quad \delta_3 = 2N^R - M^I\cdot \imath, \tag{46}$$

and equations (21) become

$$\lambda = -\mu - \nu;\ \mu = \frac{2(M^I - N^I)}{\pi}\cdot \imath;\ \nu = (\frac{3N^R}{\pi} + n) + \frac{N^I - M^I}{\pi}\cdot \imath. \tag{47}$$

For $\sigma = 0$, k^2 is positive and, as σ is decreased, k^2, likewise, decreases. When σ reaches a critical value, $\hat{\sigma}_n$, $k^2(\hat{\sigma}_n) = 0$ and thereafter continues to decrease without bound. At the critical point, $\hat{\nu} = -\frac{1+\sqrt{3}\imath}{2}\cdot \hat{\mu}$ and $\hat{N}^R =$

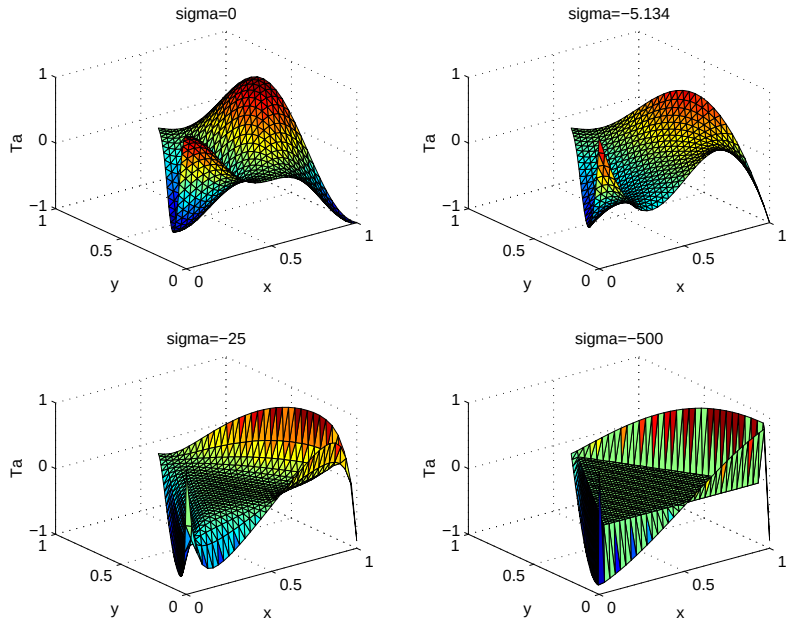

Figure 11: $(0,2)$ Antisymmetric mode

$-\frac{1}{3}[\sqrt{3}(\hat{N}^I - \hat{M}^I) + n\pi]$.

For $n = 1$, asymptotically, as $\sigma \to -\infty$, we have the limiting values:

$$M \to \tanh^{-1}(1/2) \cdot \imath;\ N \to -\frac{\pi}{3} + [\tanh^{-1}(1/2) + 3\sigma r] \cdot \imath, \tag{48}$$

$$\delta_2 \to -[\tanh^{-1}(1/2) + 6\sigma r] \cdot \imath;\ \delta_3 \to -\frac{\pi}{3} - \tanh^{-1}(1/2) \cdot \imath, \tag{49}$$

$$\mu \to -\frac{6\sigma r}{\pi} \cdot \imath\ \&\ \nu \to \frac{3\sigma r}{\pi} \cdot \imath \Rightarrow k^2 \to -4\sigma^2. \tag{50}$$

Figures 8 and 9 display $T_s^{0,1}$ and $T_a^{0,1}$, respectively, where $\hat{\sigma}_1 \approx -1.2908$. Both plots display prominent vertex singularities.

For $n > 1$, asymptotically, as $\sigma \to -\infty$, we have the limiting values:

$$M \to -[\tanh^{-1}(1/2) + \frac{3}{2}\sigma r] \cdot \imath;\ N \to -\frac{\pi}{2} - \tanh^{-1}(1/2) \cdot \imath, \tag{51}$$

$$\delta_2 \to [\tanh^{-1}(1/2) - \frac{3}{2}\sigma r] \cdot \imath;\ \delta_3 \to -\pi + [\tanh^{-1}(1/2) + \frac{3}{2}\sigma r] \cdot \imath, \tag{52}$$

$$\mu \to -\frac{3\sigma r}{\pi} \cdot \imath\ \&\ \nu \to (n - \frac{3}{2}) + \frac{3\sigma r}{2\pi} \cdot \imath \Rightarrow k^2 \to -\sigma^2 + \frac{4}{27}[\frac{\pi}{r}(n - \frac{3}{2})]^2. \tag{53}$$

Figures 10 and 11 display $T_s^{0,2}$ and $T_a^{0,2}$, respectively, where $\hat{\sigma}_2 \approx -5.134$. Both plots display prominent corner and edge singularities.

7.2.3. The (1, 1) Mode

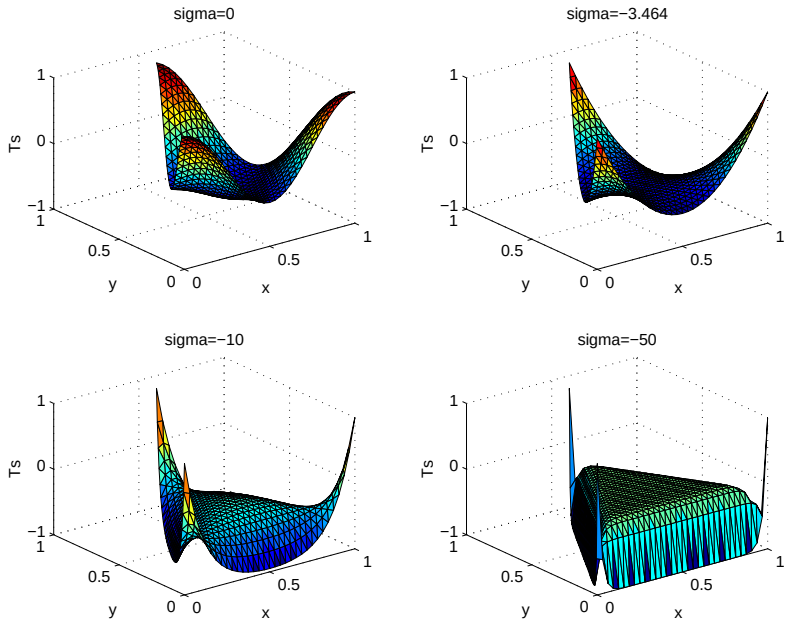

Figure 12: (1, 1) Symmetric mode

For $0 > \sigma > \tilde{\sigma} := -1/r$, we have $\mu = \nu > 0$ and the relevant equations are those of Section 5 with $m = 1$ and $n = 1$. However, when $\sigma = \tilde{\sigma} = -2\sqrt{3} \approx -3.464$ with the normalization $h = 1$, we have $\mu = \nu = 0 \Rightarrow k^2 = 0$. Also, as $\sigma \to \tilde{\sigma}$, we have $\delta_1 \to 3\pi/2$ and $\delta_2 = \delta_3 \to -\pi/2$ so that $T_s^{1,1}$ of equation (12) approaches zero. However, if we normalize $T_s^{1,1}$ so that its maximum value is one then it approaches the harmonic polynomial

$$\tilde{T}_s^{1,1} = 1 - \frac{2}{9r^3}[(r-u)^2(u+2r) + (r-v)^2(v+2r) + (r-w)^2(w+2r)]. \quad (54)$$

For $\sigma < \tilde{\sigma}$, all the parameters of Section 5 become complex:

$$\lambda = \lambda^I \cdot \imath, \quad \mu = \mu^I \cdot \imath, \quad \nu = \nu^I \cdot \imath, \quad (55)$$

$$\delta_1 = \frac{3\pi}{2} + \delta_1^I \cdot \imath, \quad \delta_2 = \delta_3 = -\frac{\pi}{2} + \delta_2^I \cdot \imath, \quad (56)$$

$$L = \frac{\pi}{2} + L^I \cdot \imath, \quad M = N = -\frac{\pi}{2} + M^I \cdot \imath. \quad (57)$$

Equation (12) becomes

$$\begin{aligned} T_s &= \sinh[\frac{\pi\lambda^I}{3r}(u+2r)-\delta_1^I]\cdot\cosh[\frac{\pi(\mu^I-\nu^I)}{9r}(v-w)] \\ &+ \sinh[\frac{\pi\mu^I}{3r}(u+2r)-\delta_2^I]\cdot\cosh[\frac{\pi(\nu^I-\lambda^I)}{9r}(v-w)] \\ &+ \sinh[\frac{\pi\nu^I}{3r}(u+2r)-\delta_3^I]\cdot\cosh[\frac{\pi(\lambda^I-\mu^I)}{9r}(v-w)], \end{aligned} \tag{58}$$

with

$$\lambda^I+\mu^I+\nu^I=0, \tag{59}$$

and eigenvalue

$$k^2=-\frac{2}{27}(\frac{\pi}{r})^2[(\lambda^I)^2+(\mu^I)^2+(\nu^I)^2]=-\frac{4}{27}(\frac{\pi}{r})^2[(\mu^I)^2+\mu^I\cdot\nu^I+(\nu^I)^2]. \tag{60}$$

Equations (19) become

$$\begin{aligned} [2L^I-M^I-N^I]\cdot\coth L^I &= -3\sigma r\,, \\ [2M^I-N^I-L^I]\cdot\coth M^I &= -3\sigma r\,, \\ [2N^I-L^I-M^I]\cdot\coth N^I &= -3\sigma r\,. \end{aligned} \tag{61}$$

Finally, equations (20) become

$$\delta_1^I=L^I-M^I-N^I;\ \delta_2^I=-L^I+M^I-N^I;\ \delta_3^I=-L^I-M^I+N^I, \tag{62}$$

and equations (21) become

$$\lambda^I=-\mu^I-\nu^I;\ \mu^I=\frac{2M^I-N^I-L^I}{\pi};\ \nu^I=\frac{2N^I-L^I-M^I}{\pi}. \tag{63}$$

Furthermore, we have $M^I=N^I$, $\delta_2^I=\delta_3^I=-L^I$, and $\mu^I=\nu^I$. Asymptotically, as $\sigma\to-\infty$, we have the limiting values:

$$L^I=-\delta_2^I=-\delta_3^I\to\frac{3}{2}\sigma r+\tanh^{-1}(1/2), \tag{64}$$

$$M^I=N^I\to\tanh^{-1}(1/2), \tag{65}$$

$$\delta_1^I\to\frac{3}{2}\sigma r-\tanh^{-1}(1/2), \tag{66}$$

$$\mu^I=\nu^I\to\frac{3\sigma r}{2\pi}\Rightarrow k^2\to-\sigma^2. \tag{67}$$

Equation (58) for $T_s^{1,1}(u,v,w)$ becomes unbounded as $\sigma\to-\infty$. However, if we first scale it by its value at a vertex, $T_s^{1,1}(r,-2r,r)$, we find that this normalized mode approaches 1 at the three vertices and 0 in the interior. The resulting edge and corner singularities are on display in Figure 12.

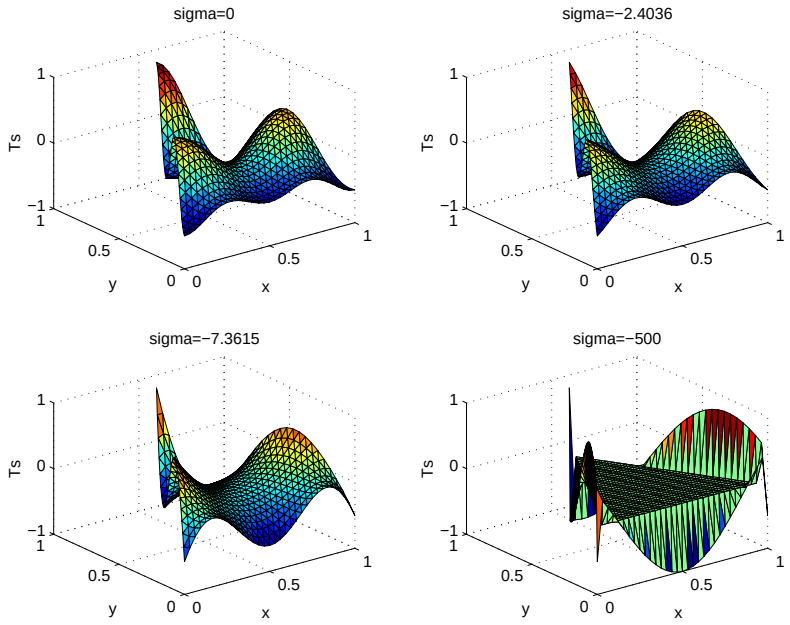

Figure 13: $(1,2)$ Symmetric mode

7.2.4. The $(1, n > 1)$ Modes

For $0 > \sigma > \sigma_n^*$, we have $\mu > 0$ and the relevant equations are those of Section 5 with $m = 1$. However, as $\sigma \to \sigma_n^*$ we have $\mu \to 0$ while $\delta_2 \to -\pi/2$ and $\delta_1 \to \delta_3 \to \pi/2$. As σ passes through σ_n^*, T_s and T_a make the transition from purely trigonometric functions to combinations of trigonometric and hyperbolic functions as in the case of the $(0, n \geq 1)$ modes.

For $\sigma < \sigma_n^*$, μ becomes pure imaginary, and the remaining parameters of Section 5 become complex in such a way so as to guarantee that k^2, T_s and T_a are real:

$$\lambda = -\nu^R - \frac{\mu^I}{2} \cdot \imath, \quad \mu = \mu^I \cdot \imath, \quad \nu = \nu^R - \frac{\mu^I}{2} \cdot \imath, \tag{68}$$

$$\delta_1 = \pi - \delta_3^R + \delta_3^I \cdot \imath, \quad \delta_2 = -\frac{\pi}{2} + \delta_2^I \cdot \imath, \quad \delta_3 = \delta_3^R + \delta_3^I \cdot \imath, \tag{69}$$

$$L = -N^R + N^I \cdot \imath, \quad M = -\frac{\pi}{2} + M^I \cdot \imath, \quad N = N^R + N^I \cdot \imath. \tag{70}$$

Note that

$$\lambda + \mu + \nu = 0. \tag{71}$$

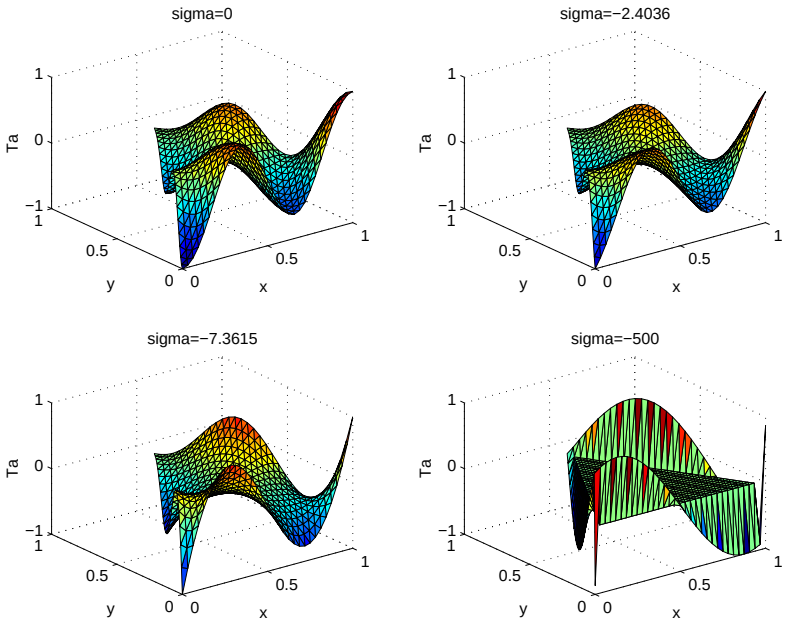

Figure 14: $(1,2)$ Antisymmetric mode

Now, the middle term of equation (12), (13) is imaginary while the outer terms are negative conjugates so that these equations may be recast in the real form

$$\begin{aligned} T_s &= \sinh[\frac{\pi\mu^I}{3r}(u+2r)-\delta_2^I]\cdot\cos[\frac{2\pi\nu^R}{9r}(v-w)] \qquad (72)\\ &+ 2\cdot\sinh[\frac{\pi\mu^I}{6r}(u+2r)+\delta_3^I]\cdot\cosh[\frac{\pi\mu^I}{6r}(v-w)]\\ &\quad\cdot\sin[\frac{\pi\nu^R}{3r}(u+2r)-\delta_3^R]\cdot\cos[\frac{\pi\nu^R}{9r}(v-w)]\\ &- 2\cdot\cosh[\frac{\pi\mu^I}{6r}(u+2r)+\delta_3^I]\cdot\sinh[\frac{\pi\mu^I}{6r}(v-w)]\\ &\quad\cdot\cos[\frac{\pi\nu^R}{3r}(u+2r)-\delta_3^R]\cdot\sin[\frac{\pi\nu^R}{9r}(v-w)],\\ T_a &= \sinh[\frac{\pi\mu^I}{3r}(u+2r)-\delta_2^I]\cdot\sin[\frac{2\pi\nu^R}{9r}(v-w)] \qquad (73)\\ &- 2\cdot\sinh[\frac{\pi\mu^I}{6r}(u+2r)+\delta_3^I]\cdot\cosh[\frac{\pi\mu^I}{6r}(v-w)] \end{aligned}$$

$$\cdot \sin[\frac{\pi\nu^R}{3r}(u+2r) - \delta_3^R] \cdot \sin[\frac{\pi\nu^R}{9r}(v-w)]$$
$$- \quad 2 \cdot \cosh[\frac{\pi\mu^I}{6r}(u+2r) + \delta_3^I] \cdot \sinh[\frac{\pi\mu^I}{6r}(v-w)]$$
$$\cdot \cos[\frac{\pi\nu^R}{3r}(u+2r) - \delta_3^R] \cdot \cos[\frac{\pi\nu^R}{9r}(v-w)]\,,$$

with eigenvalue

$$k^2 = \frac{4}{27}(\frac{\pi}{r})^2[(\nu^R)^2 - \frac{3}{4}(\mu^I)^2]. \tag{74}$$

Equations (19) become

$$-2(M^I - N^I) \cdot \coth M^I = 3\sigma r,$$
$$\frac{(3N^R + (n+\frac{1}{2})\pi)\sin(N^R)\cos(N^R) - (N^I - M^I)\sinh(N^I)\cosh(N^I)}{\cos^2(N^R)\cosh^2(N^I) + \sin^2(N^R)\sinh^2(N^I)} = 3\sigma r,$$
$$\frac{(N^I - M^I)\sin(N^R)\cos(N^R) + (3N^R + (n+\frac{1}{2})\pi)\sinh(N^I)\cosh(N^I)}{\cos^2(N^R)\cosh^2(N^I) + \sin^2(N^R)\sinh^2(N^I)}$$
$$= 0. \tag{75}$$

Finally, equations (20) become

$$\delta_1 = \frac{\pi}{2} - 2N^R - M^I \cdot \imath;$$
$$\delta_2 = -\frac{\pi}{2} + (M^I - 2N^I) \cdot \imath;\ \delta_3 = \frac{\pi}{2} + 2N^R - M^I \cdot \imath, \tag{76}$$

and equations (21) become

$$\lambda = -\mu - \nu;\ \mu = \frac{2(M^I - N^I)}{\pi} \cdot \imath;$$
$$\nu = (\frac{3N^R}{\pi} + n + \frac{1}{2}) + \frac{N^I - M^I}{\pi} \cdot \imath. \tag{77}$$

For $\sigma = 0$, k^2 is positive and, as σ is decreased, k^2, likewise, decreases. When σ reaches a critical value, $\hat{\sigma}_n < \sigma_n^*$, $k^2(\hat{\sigma}_n) = 0$ and thereafter continues to decrease without bound. At the critical point, $\hat{\nu} = -\frac{1+\sqrt{3}\imath}{2} \cdot \hat{\mu}$ and $\hat{N}^R = -\frac{1}{3}[\sqrt{3}(\hat{N}^I - \hat{M}^I) + (n+\frac{1}{2})\pi]$.

Asymptotically, as $\sigma \to -\infty$, we have the limiting values:

$$M \to -\frac{\pi}{2} + [\frac{3}{2}\sigma r + \tanh^{-1}(1/2)] \cdot \imath;\ N \to -\frac{\pi}{2} + \tanh^{-1}(1/2) \cdot \imath, \tag{78}$$
$$\delta_2 \to -\frac{\pi}{2} + [\frac{3}{2}\sigma r - \tanh^{-1}(1/2)] \cdot \imath;\ \delta_3 \to -\frac{\pi}{2} - [\frac{3}{2}\sigma r + \tanh^{-1}(1/2)] \cdot \imath, \tag{79}$$
$$\mu \to \frac{3\sigma r}{\pi} \cdot \imath\ \&\ \nu \to (n-1) - \frac{3\sigma r}{2\pi} \cdot \imath \Rightarrow k^2 \to -\sigma^2 + \frac{4}{27}[\frac{\pi}{r}(n-1)]^2. \tag{80}$$

Figures 13 and 14 display $T_s^{1,2}$ and $T_a^{1,2}$, respectively, where $\sigma_2^* \approx -2.4036$ and

$\hat{\sigma}_2 \approx -7.3615$. Both plots display prominent vertex and edge singularities.

8. Spectral Properties

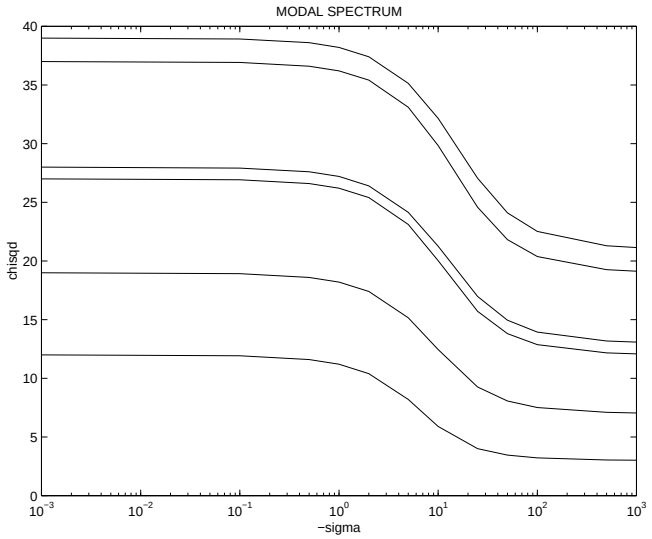

Figure 15: Spectral parameter: ABC-dirichlet modes

The modal frequencies, $f_{m,n}$, are proportional to the square root of the eigenvalues given by equation (15). Hence, we have

$$f_{m,n} \propto \frac{4\pi}{3h}\chi;\ \chi^2 := \mu^2 + \mu\nu + \nu^2. \tag{81}$$

Thus, the spectral structure, real or imaginary, of the equilateral triangle hinges upon the properties of the spectral parameter χ^2.

This spectral parameter as σ ranges from 0 to $-\infty$ is shown in Figure 15 for the first six ABC-Dirichlet modes: the $(2,2)$, $(2,3)$, $(3,3)$, $(2,4)$, $(3,4)$ and $(2,5)$ modes in order of increasing χ^2. The left side corresponds to the Neumann modes ($\sigma = 0$) and the right side corresponds to the Dirichlet modes ($\sigma = -\infty$). Thus, this figure graphically displays the homotopy relating these two well understood eigenvalue problems. Likewise, Figure 16 displays the cube root of the spectral parameter for the first six missing modes: the $(0,0)$, $(0,1)$, $(1,1)$, $(0,2)$, $(1,2)$ and $(0,3)$ modes also in order of increasing χ^2. Since $n^2 < 1+n+n^2 < (n+1)^2$ for $n \geq 1$, the interleaving of $(0,n)$ and $(1,n)$ modes present in Figure 16 persists as $n \to \infty$.

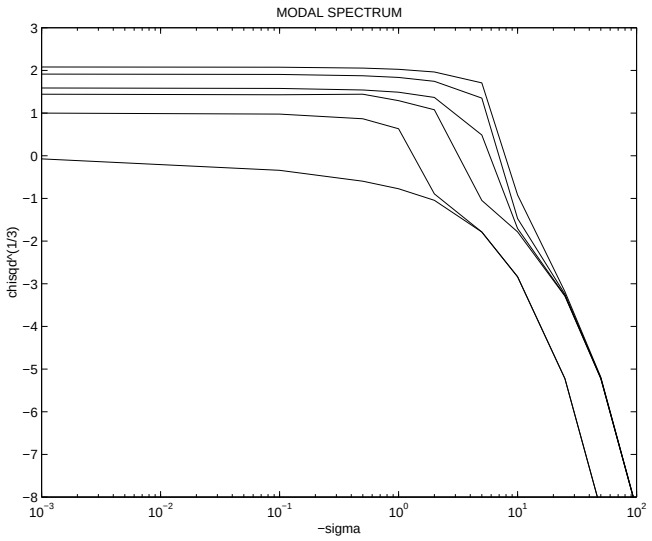

Figure 16: Spectral parameter: missing modes

Since $T_s^{m,n}$ and $T_a^{m,n}$ both correspond to the same frequency $f_{m,n}$ given by equation (81), it follows that all eigenvalues corresponding to $m \neq n$ have multiplicity equal to at least two. However, this modal degeneracy, as it is known in the engineering literature, extends also to the case $m = n$. Additional modal degeneracy is manifested by the intersection of two modal curves. For the Dirichlet and Neumann problems, number theoretic techniques permit a comprehensive treatment of such spectral multiplicity, [10].

However, for the Robin problem with either radiation or absorbing boundary condition, μ and ν are not integers and such techniques fail. At the present time, no general results are available and one must resort to perusal of Figure 15, suitably extended, in order to locate ABC-Dirichlet modal degeneracies for $0 > \sigma > -\infty$. All one can say with certainty is that if $(m_1 \geq 2, n_1)$ and $(m_2 \geq 2, n_2)$ are modal indices satisfying the inequalities

$$0 < (m_2^2 + m_2 n_2 + n_2^2) - (m_1^2 + m_1 n_1 + n_1^2) < 3[(m_2 + n_2) - (m_1 + n_1)]\,, \quad (82)$$

then the corresponding modal curves must intersect for some value of σ which will thereby generate a corresponding modal degeneracy. For example, this inequality reveals that the $(2, 11)$ and $(6, 8)$ modes must be degenerate for some intermediate value of σ.

As Figure 16 indicates, the modal curves corresponding to missing modes never intersect (except possibly at infinity). However, if we were to super-

impose Figure 16 upon Figure 15 then the $(0, n \geq 4)$ and $(1, n \geq 3)$ modal curves would intersect with those of ABC-Dirichlet modes thereby generating additional degeneracies.

9. Orthogonality and Completeness

By Rellich's Theorem, see [6], eigenfunctions corresponding to distinct eigenvalues are guaranteed to be orthogonal. Also, a symmetric mode and an antisymmetric mode are automatically orthogonal. However, as we discovered above, the multiplicity of the eigenvalues given by equation (15) is quite a complicated matter. Thus, we invoke the following continuity argument in order to confirm the orthogonality of our collection of eigenfunctions $\{T_s^{m,n}\ (n \geq m \geq 0);\ T_a^{m,n}\ (n > m \geq 0)\}$.

Suppose that f and g are eigenfunctions of like parity that share an eigenvalue, k^2, for some fixed value of $\sigma = \hat{\sigma}$. This corresponds to an intersection of two spectral curves. For σ in the neighborhood of $\hat{\sigma}$, Rellich's Theorem guarantees that $\langle f, g \rangle = \int\int_\tau fg\ dA = 0$. Thus, by continuity, $\langle f, g \rangle = 0$ for $\sigma = \hat{\sigma}$ and orthogonality of our full collection of ABC modes is assured.

It is not *a priori* certain that the collection of eigenfunctions $\{T_s^{m,n},\ T_a^{m,n}\}$ constructed above is complete. For domains which are the Cartesian product of intervals in an orthogonal coordinate system, such as rectangles and annuli, completeness of the eigenfunctions formed from products of one-dimensional counterparts has been established, see [13]. Since the equilateral triangle is not such a domain, we must employ other devices in order to establish completeness.

We will utilize an analytic continuation argument which hinges upon the previously established completeness of the Neumann modes [12]. The homotopy between the Neumann and ABC modes that we have established above guarantees a unique branch leading from each of the Neumann modes to its corresponding ABC mode. Likewise, for any $-\infty < \sigma < 0$ we may trace out a branch from any mode leading back to a Neumann mode as $\sigma \to 0^-$.

Suppose, for the sake of argument, that the collection of ABC modes constructed above is not complete for some $-\infty < \sigma = \hat{\sigma} < 0$. Then, let $u(x, y; \hat{\sigma})$ be a mode that is not contained in our collection. As we have a self-adjoint operator, there exist ℓ analytic branches emanating from this point in Hilbert space where ℓ is the multiplicity of $k^2(\hat{\sigma})$, see [1]. Denote any of these branches, analytically continued back to $\sigma = 0$ as $u(x, y; \sigma)$. Since we know that the collection of Neumann modes is complete, this branch must at some point, $\sigma = \sigma^*$, coalesce with a branch emanating from one of our ABC modes.

However, as we now show, the analytic dependence of $u(x,y;\sigma)$ upon σ precludes such a bifurcation at $\sigma = \sigma^*$. To see this, let

$$\Delta u + k^2 u = 0,\ (x,y) \in \tau;\ \frac{\partial u}{\partial \nu} + \sigma u = 0,\ (x,y) \in \partial\tau. \tag{83}$$

Then

$$u(x,y;\sigma) = u(x,y;\sigma^*) + u'(x,y;\sigma^*)\cdot(\sigma - \sigma^*) + u''(x,y;\sigma^*)\cdot\frac{(\sigma-\sigma^*)^2}{2} + \cdots, \tag{84}$$

where $u' := \frac{\partial u}{\partial \sigma}$ and each of the correction terms in the Taylor series is orthogonal to the eigenspace of $k^2(\sigma^*)$.

Each of the Taylor coefficients satisfies the boundary value problem

$$\Delta u^{(n)}(x,y;\sigma^*) + k^2(\sigma^*)u^{(n)}(x,y;\sigma^*) = 0,\ (x,y) \in \tau, \tag{85}$$

$$\frac{\partial u^{(n)}}{\partial \nu}(x,y;\sigma^*) + \sigma^* u^{(n)}(x,y;\sigma^*) = -n u^{(n-1)}(x,y;\sigma^*),\ (x,y) \in \partial\tau,$$

which may be solved recursively and uniquely for $u', u'', \ldots, u^{(n)}, \ldots$ since they are each orthogonal to the eigenspace of k^2. Thus, $u(x,y;\sigma)$ is uniquely determined and bifurcation cannot transpire. Consequently, our collection of ABC modes is indeed complete.

10. Conclusion

In the foregoing, we have filled a prominent gap in the applied mathematical literature by providing a complete elementary derivation of the extension of Lamé's formulas for the eigenfunctions of the equilateral triangle to the absorbing boundary condition. In addition to its innate mathematical interest, this problem is of practical interest as it relates to the calibration of numerical algorithms for approximating the eigenvalues of the Laplacian upon triangulated domains.

The preceding analysis reveals a partial analogy to the case of the radiation boundary condition [9] in that a subset of the the ABC modes associated with nonnegative eigenvalues, the ABC-Dirichlet modes, lie along a homotopic path leading from a Neumann mode [8] to a Dirichlet mode [7]. The bulk of this paper has been devoted to exploring the nature of the remaining missing modes associated with eigenvalues which migrate towards negative infinity.

In addition, we have established the orthogonality and completeness of this collection of eigenfunctions using the simplest of mathematical tools. Furthermore, we have made an extensive investigation of the properties of the spectrum and modes. The final installment of this series of papers on the eigenstructure

of the equilateral triangle will treat the so-called impedance boundary condition (σ complex) which arises in the analysis of waveguide problems where the propagating wave penetrates the walls of the guiding structure.

Acknowledgements

The author thanks Mrs. Barbara A. McCartin for her indispensable aid in constructing the figures. This paper is dedicated to the memory of my beloved brother Dennis A. McCartin (MST, CPA).

References

[1] K.O. Friedrichs, *Perturbation of Spectra in Hilbert Space*, American Mathematical Society, Providence RI (1965), 92-94.

[2] J. Gray, Möbius's geometrical mechanics, In: *Möbius and His Band* (Ed-s: J. Fauvel et al) Oxford, New York, NY (1993).

[3] G. Lamé, Mémoire sur la propagation de la chaluer dans les polyèdres, *Journal de l'École Polytechnique*, **22** (1833), 194-251.

[4] G. Lamé, *Leçons sur la Théorie Analytique de la Chaleur*, Mallet-Bachelier, Paris (1861).

[5] G. Lamé, *Leçons sur la Théorie Mathématique de l'Élasticité des Corps Solides*, Deuxième Édition, Gauthier-Villars, Paris (1866).

[6] C. R. MacCluer, *Boundary Value Problems and Orthogonal Expansions: Physical Problems from a Sobolev Viewpoint*, IEEE Press, New York, NY (1994).

[7] B.J. McCartin, Eigenstructure of the equilateral triangle, Part I: The Dirichlet problem, *SIAM Review*, **45**, No. 2 (2003), 267-287.

[8] B.J. McCartin, Eigenstructure of the equilateral triangle, Part II: The Neumann problem, *Mathematical Problems in Engineering*, **8**, No. 6 (2002), 517-539.

[9] B.J. McCartin, Eigenstructure of the equilateral triangle, Part III: The Robin problem, *International Journal of Mathematics and Mathematical Sciences*, **2004**, No. 16 (16 March 2004), 807-825.

[10] B.J. McCartin, Modal degeneracy in equilateral triangular waveguides, *J. Electromagnetic Waves and Applications*, **16**, No. 7 (2002), 943-956.

[11] F. Pockels, *Über die Partielle Differentialgleichung* $\Delta u + k^2 u = 0$, B.G. Teubner, Leipzig (1891).

[12] M. Práger, Eigenvalues and eigenfunctions of the Laplace operator on an equilateral triangle, *Applications of Mathematics*, **43**, No. 4 (1998), 311-320.

[13] W.A. Strauss, *Partial Differential Equations: An Introduction*, Wiley, New York, NY (1992).